Eur. Phys. J. C 55, 653–665 (2008)
DOI 10.1140/epjc/s10052-008-0617-3

THE EUROPEAN PHYSICAL JOURNAL C

Regular Article – Theoretical Physics

Charged Higgs bosons in the next-to MSSM (NMSSM)

A.G. Akeroyd[1,2], A. Arhrib[3,4], Qi-Shu Yan[5,a]

[1] Department of Physics, National Cheng Kung University, Tainan 701, Taiwan, R.O.C.
[2] National Center for Theoretical Sciences, Hsinchu, Taiwan, R.O.C.
[3] Department of Physics, National Central University, Chung Li, Taiwan, R.O.C.
[4] Département de Mathématiques, Faculté des Sciences et Techniques, B.P. 416, Tangier, Morocco
[5] Department of Physics, National Tsing Hua University, 101, Section 2, Guang Fu Road, Hsinchu, Taiwan, R.O.C.

Received: 1 February 2008 /
Published online: 17 May 2008 –

Abstract. The charged Higgs boson decays $H^\pm \to W^\pm A_1$ and $H^\pm \to W^\pm H_i$ are studied in the framework of the next-to-minimal supersymmetric standard model (NMSSM). It is found that the decay rate for $H^\pm \to W^\pm A_1$ can exceed the rates for the $\tau^\pm\nu$ and tb channels both below and above the top–bottom threshold. The dominance of $H^\pm \to W^\pm A_1$ is most readily achieved when A_1 has a large doublet component and small mass. We also study the production process $pp \to H^\pm A_1$ at the LHC followed by the decay $H^\pm \to W^\pm A_1$, which leads to the signature $W^\pm A_1 A_1$. We suggest that $pp \to H^\pm A_1$ is a promising discovery channel for a light charged Higgs boson in the NMSSM with small or moderate $\tan\beta$ and dominant decay mode $H^\pm \to W^\pm A_1$. This $W^\pm A_1 A_1$ signature can also arise from the Higgsstrahlung process $pp \to W^\pm H_1$ followed by the decay $H_1 \to A_1 A_1$. It is shown that there exist regions of parameter space where these processes can have comparable cross sections and we suggest that their respective signals can be distinguished at the LHC by using appropriate reconstruction methods.

PACS. 12.60.Fr; 14.80.Cp

1 Introduction

An attractive extension of the minimal supersymmetric standard model (MSSM) is the next-to MSSM (NMSSM), in which an additional singlet neutral complex scalar field S is added. The presence of this singlet field provides an elegant solution to the μ problem of the MSSM. The μ parameter in the MSSM superpotential, which does not break supersymmetry (SUSY) and is present when SUSY is unbroken, is completely unrelated to the electroweak or SUSY breaking scales. In some models like supergravity, μ is naturally expected to be of the order $M_{\rm Planck}$. However, the radiative electroweak symmetry breaking conditions require the μ parameter to be of the same order as M_Z. Such a conflict is called the μ problem [1–3].

The superpotential of the NMSSM contains the term $\lambda \hat{S}\hat{H}_u\hat{H}_d$, and the μ term of the MSSM, which mixes the two doublet fields $\hat{H}_u$ and $\hat{H}_d$, is not present explicitly. When the singlet field acquires a vacuum expectation value $\langle s \rangle$ of the order of the SUSY breaking scale, an effective μ parameter $\mu_{\rm eff} = \lambda s$ of the order of the electroweak scale is then dynamically generated. Moreover, it has been shown that with the additional singlet Higgs field the MSSM fine-tuning (or "little hierarchy problem") problem can be ameliorated in regions of the NMSSM parameter space [4, 5].

A charged Higgs boson ($H^\pm$) appears in any extension of the standard model with two hypercharge $Y = 1$ doublets. Its phenomenology has been extensively studied in both the two Higgs doublet model (2HDM) and MSSM. The phenomenology of $H^\pm$ in the NMSSM is similar in many ways to that in the MSSM, since no charged singlet fields have been added. The increased parameter content of the NMSSM scalar potential compared to that of the MSSM permits large mass splittings among the Higgs spectrum, which allows other decay modes of $H^\pm$ to be important that were substantially suppressed in the context of the MSSM. In the MSSM the coupling $H^\pm A\, W$ (where A is the CP-odd neutral Higgs boson) contains no mixing angle suppression but the relation $M_A \sim M_{H^\pm}$ ensures that the decay $H^\pm \to A\, W$ is greatly suppressed in most of the parameter space [6–8]. In the NMSSM there are two pseudoscalars A_1 and A_2, which are mixtures of the doublet and singlet fields. There exist regions in the theoretical parameter space where A_1 is predominantly doublet and light, and hence the decay $H^\pm \to A_1 W$ is unsuppressed.

The importance of the decay $H^\pm \to A_1 W$ in the NMSSM was emphasized in [9] where it was shown that dominance over $H^\pm \to cs, \tau\nu$ is possible, and branching ratios close to 100% can be attained for intermediate values

[a] e-mail: yanqs@phys.nthu.edu.tw

of $\tan\beta$. A LHC simulation was performed in [10] and it was concluded that such a decay offers very good detection prospects for $H^\pm$ if the branching ratios of $t \to H^\pm b$ and $H^\pm \to A_1 W$ are sufficiently large. In this work we perform a comprehensive scan of the NMSSM parameter space using the publicly available code NMHDECAY [11, 12] in order to identify the regions where $H^\pm \to A_1 W$ can be sizeable.

The strength of the coupling $H^\pm A_1 W$ can also have an application to the production of $H^\pm$ via $pp \to H^\pm A_1$, which has been studied in the CP conserving MSSM [13–15] and CP violating MSSM [16]. If the branching ratio for the decay $H^\pm \to A_1 W$ were also sizeable such a production mechanism would lead a final state of $Wbbbb$ (for $M_{A_1} > 2m_b$) [16], which has been simulated [17] in the context of the LHC with promising conclusions. This $Wbbbb$ signature can also arise from the process $pp \to W H_1 \to W A_1 A_1$, which was simulated in [18] and shown to provide a clear signal at the LHC. We compare the magnitude of both mechanisms and discuss how they may be distinguished.

Our work is organized as follows: in Sect. 2 we present a short review of the Higgs sector of the NMSSM; in Sect. 3 the limits that lead to a light A_1 in the NMSSM parameter space are listed; in Sect. 4 the phenomenology of $H^\pm$ is introduced; Sect. 5 contains our numerical results for the branching ratios of $H^\pm \to A_1 W, H_1 W$ and cross sections $pp \to H^\pm A_1 \to Wbbbb(W\tau\tau\tau\tau)$ and $pp \to W H_1 \to Wbbbb(W\tau\tau\tau\tau)$. Conclusions are given in Sect. 6.

2 A brief review on the Higgs sector of the NMSSM

For detailed discussions of the Higgs sector of the NMSSM the reader is referred to [19–23]. In this section we follow the notation of [24]. The NMSSM Higgs sector differs from that of the MSSM by the addition of an extra complex scalar field, S. The Higgs fields of the model then consist of the usual two Higgs doublets $\hat{H}_u$ and $\hat{H}_d$ together with this extra Higgs singlet.

In the NMSSM Lagrangian, the extra singlet field is allowed to couple only to the Higgs doublets of the model and consequently the couplings of the new field S to gauge bosons and fermions will only be manifest via their mixing with the doublet Higgs fields. The superpotential of the NMSSM is given by

$$W = W_{\rm MSSM} + \lambda \hat{S} \hat{H}_u \hat{H}_d + \frac{1}{3}\kappa \hat{S}^3 \,, \tag{1}$$

where $W_{\rm MSSM}$ is the usual MSSM superpotential and only terms that depend on the singlet field are explicitly written. The soft breaking terms for both the doublet and singlet are included in $V_{\rm soft}$:

$$\begin{aligned} V_{\rm soft} = {} & m_{H_u}^2 |H_u|^2 + m_{H_d}^2 |H_d|^2 + m_S^2 |S|^2 \\ & + \left[\lambda A_\lambda S H_u H_d + \frac{1}{3}\kappa A_\kappa S^3 + {\rm h.c.} \right] . \end{aligned} \tag{2}$$

The parameters additional to those of the MSSM are λ, κ, A_λ, A_κ, m_S and the vacuum expectation value of the singlet field, s, which will generate the effective μ term given by $\mu_{\rm eff} = \lambda s$. As in the MSSM, m_S can be fixed by the minimization condition of the scalar potential.

After electroweak symmetry breaking the Higgs spectrum of the NMSSM consists of three neutral scalars (H_1, H_2, H_3), two pseudoscalars (A_1, A_2) and a pair of charged Higgs bosons $H^\pm$. In both the CP-odd and CP-even sector the physical eigenstates are ordered as $M_{H_1} \lesssim M_{H_2} \lesssim M_{H_3}$ and $M_{A_1} \lesssim M_{A_2}$. The mass of $H^\pm$ at tree level is given by [19, 25]

$$M_{H^\pm}^2 = \frac{2\mu_{\rm eff}}{\sin 2\beta}(A_\lambda + \kappa s) + M_W^2 - \lambda^2 v^2 \,, \tag{3}$$

where $\tan\beta = v_u/v_d$ and $v^2 = v_u^2 + v_d^2$. This differs from the corresponding MSSM expression, in which M_A and $M_{H^\pm}$ are strongly correlated and become roughly equal for $M_A \geq 140\,{\rm GeV}$.

The CP-odd mass matrix can be obtained as follows: firstly, as in MSSM one rotates the bare fields $(\Im m H_u, \Im m H_d, \Im m S)$ into a basis $(A, G, \Im m S)$ where G is a massless Goldstone boson. Then one eliminates the Goldstone mode, and the remaining 2×2 CP-odd mass matrix in the basis $(A, \Im m S)$ is given by

$$\begin{aligned} \mathcal{M}_{P,11}^2 &= \frac{\lambda s}{\sin\beta\cos\beta}(A_\lambda + \kappa s) \,, \\ \mathcal{M}_{P,22}^2 &= \left(2\lambda\kappa + \frac{\lambda A_\lambda}{2s} \right) \sin 2\beta v^2 - 3\kappa A_\kappa s \,, \\ \mathcal{M}_{P,12}^2 &= \lambda v (A_\lambda - 2\kappa s) \,. \end{aligned} \tag{4}$$

Here $A = \cos\beta \Im m H_u + \sin\beta \Im m H_d$ is the CP-odd MSSM Higgs boson, while $\Im m S$ comes from the singlet S field. The pseudoscalar fields are further rotated to the diagonal basis (A_1, A_2) by an orthogonal 2×2 matrix such that

$$\begin{aligned} A_1 &= \cos\theta_A \; A + \sin\theta_A \Im m(S) \\ A_2 &= -\sin\theta_A \; A + \cos\theta_A \Im m(S) \,, \end{aligned} \tag{5}$$

where

$$\begin{aligned} \cos\theta_A &= \frac{\mathcal{M}_{P,12}^2}{\sqrt{\mathcal{M}_{P,12}^4 + \left(M_{A_1}^2 - \mathcal{M}_{P,11}^2 \right)^2}} \,, \\ \sin\theta_A &= \frac{M_{A_1}^2 - \mathcal{M}_{P,11}^2}{\sqrt{\mathcal{M}_{P,12}^4 + \left(M_{A_1}^2 - \mathcal{M}_{P,11}^2 \right)^2}} \,. \end{aligned} \tag{6}$$

The Higgs boson–gauge boson couplings originate from the covariant derivative of the kinetic energy term. Those relevant for our study are described by the following Lagrangian:

$$\begin{aligned} \mathcal{L}_{VVH,VHH} = {} & g m_W g_{VVH_i} W^{+\mu} W_\mu^- H_i \\ & - g W_\mu^+ \left(\frac{{\rm i} g_{W^+H^-H_i}}{2} H_i + \frac{P_{i1}}{2} A_i \right) \overset{\leftrightarrow\mu}{\partial} H^- + {\rm h.c.} \,, \end{aligned} \tag{7}$$

where $g_{VVH_i} = \sin\beta S_{i1} + \cos\beta S_{i2}$, $g_{W^+H^-H_i} = \cos\beta S_{i1} - \sin\beta S_{i2}$, $P_{11} = \cos\theta_A$ and $P_{21} = -\sin\theta_A$; S and P are orthogonal matrices that diagonalize respectively the CP-even and CP-odd scalar mass matrix. From the last term in (7) one can see that the vertex $W^{\pm}H^{\mp}A_1$ is directly proportional to P_{11} i.e. the doublet component of the mass eigenstate A_1. Consequently, if A_1 is entirely composed of doublet fields this coupling is maximized, and if A_1 is purely singlet the coupling vanishes.

As in the MSSM one can easily derive the following sum rules:

$$\sum_{i=1}^{3} g^2_{WWH_i} = 1\,,$$
$$g^2_{WWH_i} + g^2_{W^+H^-H_i} + S^2_{i3} = 1\,, \quad i = 1,2,3\,. \tag{8}$$

Here S_{i3} is the singlet component of H_i. From the second sum rule it follows that if H_i is purely doublet ($S_{i3} \approx 0$) then the MSSM sum rule, $g^2_{WWH_i} + g^2_{W^+H^-H_i} = 1$, is recovered, where H_i is entirely composed of doublet fields. Conversely, if H_i is purely singlet ($S^2_{i3} \approx 1$), then one has $g^2_{WWH_i} + g^2_{W^+H^-H_i} \approx 0$ and both H_iVV and $H_iH^+W^-$ must be suppressed, and this will present a real challenge for the detection of Higgs bosons. This sum rule will be explored in our numerical analysis.

3 A light A_1 in the NMSSM parameter space

The parameter space of the NMSSM can naturally accommodate a light A_1, which is of great phenomenological interest. To identify such regions it is instructive to examine the vanishing limits of the determinant of the mass matrix of the pseudoscalar, which can be expressed as

$$\det M_P^2 = -\frac{3\kappa\lambda s}{\sin 2\beta}\left(2\kappa s^2 A_\kappa + 2sA_\kappa A_\lambda - 3\lambda A_\lambda v^2 \sin 2\beta\right). \tag{9}$$

It is then straightforward to identify four distinct cases where $\det M_P^2$ approaches 0:

- Case 1: $A_\lambda \to 0$ and $A_\kappa \to 0$ [26];
- Case 2: $\kappa \to 0$ [27–30];
- Case 3: $\lambda \to 0$;
- Case 4: $s \to 0$.

Moreover, it is evident that combinations of these basic cases can also lead to a light A_1. The requirement of perturbativity up to the grand unification scale restricts $\lambda < 0.8$ [31, 32]. Therefore, case 4 ($s \to 0$) is ruled out, since it would lead to a very small $\mu_{\rm eff}$, which is excluded by the mass bound for charginos from direct searches. However, if one gives up this perturbative requirement up to the grand unification scale and considers $\lambda \gg 1$, as in the so-called λSUSY model [33] (which can be realized in supersymmetric fat Higgs models [34–37]), then case 4 might be viable.

The first two limits are related with the discrete symmetries of the Higgs potential: one is called the R-axion limit with $A_\lambda \to 0$ and $A_\kappa \to 0$ [26]; the other is called the PQ-axion limit with $\kappa \to 0$ the superpotential (1) and its associated Lagrangian contains an extra global U(1) symmetry [27–30]. In both cases, these symmetries are spontaneously broken by the Higgs vev leading to a pseudo-Goldstone boson in the spectrum.

At tree level, in the R-axion limit [26], the mass spectra and mixing of the CP-odd Higgs sector can be expressed as

$$\begin{aligned} m^2_{A_1} &= 3s\left(-\kappa A_\kappa \sin^2\theta_A + \frac{3}{2\sin 2\beta}\lambda A_\lambda \cos^2\theta_A\right) \\ &\quad + O\left(\kappa^2 A^2_\kappa, \lambda^2 A^2_\lambda\right), \\ m^2_{A_2} &= \frac{2\lambda\kappa v^2}{\cos^2\theta_A}\sin 2\beta + O\left(\kappa^2 A^2_\kappa, \lambda^2 A^2_\lambda\right), \\ \tan\theta_A &= \frac{s}{v\sin 2\beta} + O\left(\kappa A_\kappa, \lambda A_\lambda\right). \end{aligned} \tag{10}$$

In the R-axion limit scenario, as can be seen from (10), a light pseudoscalar is obtained for small κA_κ and λA_λ or a combination of small κA_κ and λA_λ.

At tree level, in the PQ-axion limit [27–30], one has

$$\begin{aligned} m^2_{A_1} &= 3s\kappa\left(-A_\kappa \sin^2\theta_A + \frac{6}{\sin 2\beta}\lambda s \cos^2\theta_A\right) + O\left(\kappa^2\right), \\ m^2_{A_2} &= -\frac{2\lambda A_\lambda v}{\sin 2\theta_A} + O\left(\kappa^2\right), \\ \tan\theta_A &= -\frac{2s}{v\sin 2\beta} + O\left(\kappa\right). \end{aligned} \tag{11}$$

It is interesting to see that in (11) the limit $\kappa \to 0$ gives $m_{A_1} \to 0$. This is actually the case where the U(1) PQ symmetry is left unbroken in the superpotential. The spontaneous breaking of such PQ symmetry by a Higgs vev leads to a massless Goldstone boson, the axion. To obtain a light pseudoscalar A_1, one needs to introduce a small κ that only slightly breaks the PQ symmetry.

The third case is also related with a discrete symmetry of two Higgs doublet models. In this limit one has

$$\begin{aligned} m^2_{A_1} &= \frac{2\lambda s}{\sin 2\beta}(A_\lambda + \kappa s) + O(\lambda^2), \\ m^2_{A_2} &= -3\kappa s A_\kappa + O(\lambda), \\ \tan\theta_A &= \lambda\frac{(A_\lambda - 2\kappa s)v}{3\kappa A_\kappa s} + O(\lambda^2). \end{aligned} \tag{12}$$

When $\lambda \to 0$, a large value for s is needed to keep $\mu_{\rm eff}$ of the order of the electroweak scale. In this case A_1 is mainly doublet and this is the exact MSSM limit.

4 $H^{\pm}$ in the NMSSM

In this section we describe the phenomenology of the $H^{\pm}$ in the NMSSM and highlight its differences with the phenomenology of $H^{\pm}$ in the MSSM. The phenomenology of $H^{\pm}$ in the NMSSM has many similarities with that of $H^{\pm}$ in the MSSM (the latter recently reviewed in [38]). This

is to be expected since the fermionic couplings are identical in the two models. The main differences in their phenomenology originate from the possibility of large mass splittings among the Higgs bosons in the NMSSM, which permits decay channels like $H^\pm \to A_1 W$ to proceed on-shell [9]. In the MSSM such a decay can only be open for extreme choices of certain SUSY parameters (e.g. for $\mu > 4M_{\rm SUSY}$ [39,40]), which induce large quantum corrections in the effective scalar potential. Moreover, in the NMSSM a light CP-even H_1 is also allowed and one can have the opening of the decay $H^\pm \to H_1 W$ both below and above the top–bottom threshold. This latter channel may change the NMSSM phenomenological predictions for the charged Higgs with respect to the MSSM [9]. In the MSSM the decay $H^\pm \to H_1 W$ is also open but the coupling $g_{W^+H^-H_1} \sim \cos^2(\beta-\alpha)$ is strongly suppressed when $M_{H^\pm} \gg m_{H_1} + m_W$ and thus its branching ratio is very small for such $M_{H^\pm}$. For $M_{H^\pm} < m_{H_1} + m_W$ and just above the threshold the branching ratio for this channel can reach 10% at most for small values of $\tan\beta$ [6–8,10].

The phenomenology of $H^\pm$ in the NMSSM has received considerably less attention than its neutral Higgs sector. In recent years much effort has been focused on establishing a "no–lose theorem" at the LHC in which detection of at least one Higgs boson in the NMSSM is guaranteed. However, the potential importance of the decay $H_1 \to A_1 A_1$ [26,41,42] has prevented such a theorem from being established [24,43–46]. Moreover, it has been shown that a large branching ratio for $H_1 \to A_1 A_1$ would weaken the LEP bounds for a SM like H_1 in the NMSSM [4].

For $M_{A_1} < 2m_b$ [5,47,48], dominance of $H_1 \to A_1 A_1$ has the virtue of allowing H_1 to be as light as $90 \to 100$ GeV and can realize the "LEP excess scenario" easily. Such values of M_{H_1} can be accommodated in the NMSSM with little fine-tuning, in contrast to the MSSM case where considerable fine-tuning is necessary in order to comply with the LEP limit $M_{H_1} > 114$ GeV from the Higgsstrahlung channel. However, a large branching ratio for $H_1 \to A_1 A_1$ followed by $A_1 A_1 \to 4\tau$ is challenging for detection at the Tevatron [49]. For the final states $V2b2\tau$ and $V4b$ at the Tevatron, the observation is difficult due to the limited statistics, as shown in [50]. At the LHC, by utilizing the central exclusive production process and high-resolution low-angle sub-detectors, it is shown in [51] that it is possible to reconstruct the masses of H_1 and A_1. In [52] it was suggested that production of A_1 in association with charginos followed by the possibly dominant decay $A_1 \to \gamma\gamma$ could offer good detection prospects for an almost purely singlet A_1. An alternative probe is the decay $\Upsilon \to A_1\gamma$ at B factories [53,54]. A high-energy e^+e^- linear collider would easily probe the scenario of dominant decay $H_1 \to A_1 A_1$ for $m_{A_1} < 2m_b$ via the recoil mass technique, which is insensitive to the decay of H_1.

For $M_{A_1} > 2m_b$ one would have the dominant decay $A_1 A_1 \to bbbb$, for which a LEP limit of $M_{H_1} > 110$ GeV was derived. In such a scenario the fine-tuning problem is not greatly ameliorated, but detection prospects at the LHC are much better. In partonic level analyses it has been shown that a signal with high significance and full Higgs mass reconstruction can be obtained from the process $pp \to W H_1 \to W A_1 A_1 \to W bbbb$ [18,50]. The main challenge in reconstructing the full decay chain is to retain an adequate tagging efficiency of the b in the low $p_{\rm T}$ region where signal events are located, as shown in [50].

In many of the studies that are concerned with establishing a no-lose theorem the charged Higgs mass is taken to be very heavy $M_{H^\pm} > 400$ GeV (e.g. the benchmark points in [45]). It has been known for some time that a moderately light $M_{H^\pm} < m_t$ is possible in the NMSSM. A first detailed study appeared in [9], and this possibility has been recently emphasized in [55]. However, such a $H^\pm$ would contribute sizably to the rare decay $b \to s\gamma$ whose branching ratio has been measured and is consistent with the SM expectation. In the context of the NMSSM a contribution to $b \to s\gamma$ from another new physics particle (usually the lightest chargino, $\chi_1^\pm$) is needed to partially cancel the large $H^\pm$ contribution for $M_{H^\pm} < m_t$ [56,57]. If flavor violation induced by gluinos ($\tilde{g}$) is considered [58], the NMSSM parameter space for a light $H^\pm$ can be enlarged, while keeping the branching ratio for $b \to s\gamma$ consistent with the measured value. This merely requires a suitable cancellation among the contributions from $H^\pm$, $\chi_1^\pm$ and $\tilde{g}$, the latter being of essentially arbitrary magnitude. In light of this possibility we do not impose the $b \to s\gamma$ constraint in our numerical analysis.

Another potentially important constraint on the scenario of $M_{H^\pm} \lesssim m_t$ comes from the measurement of the decay $B^\pm \to \tau^\pm \nu$ [59–61]. This decay is mediated at tree level [62] by $H^\pm$, and its contribution cannot be canceled by any other new particle in the model. Current data exclude two regions in the parameter space of $[M_{H^\pm}, \tan\beta]$. However, the non-holomorphic contribution [63–65] would shift the location of these two regions and thus we do not impose such a constraint in our analysis. Importantly, for $\tan\beta \lesssim 20$, of most interest to us, $M_{H^\pm} \lesssim m_t$ is almost always allowed. Moreover, a recent analysis [66] shows that a light charged Higgs boson in the NMSSM is compatible with the constraints from $b \to s\gamma$, ΔM_q, $B^\pm \to \tau^\pm\nu$ and $B_s \to \mu^+\mu^-$ even without invoking extra sources of flavor violation from gluinos.

5 Charged Higgs decay $H^\pm \to SW$ and the production mechanism $pp \to H^\pm S$, $S = A_1, H_1$

5.1 Charged Higgs decay modes $H^\pm \to SW$

The decay $H^\pm \to A\,W$, where A is a CP-odd Higgs boson, may be sizeable in a variety of models with a non-minimal Higgs sector such as two Higgs doublet models (Type I and II) [67–71] and in SUSY models with Higgs triplets [72]. Two LEP collaborations (OPAL and DELPHI) performed a search for a charged Higgs decaying to $A\,W^*$ (assuming $m_A > 2m_b$) and derived limits on the charged Higgs mass [73–75] comparable to those obtained from the search for $H^\pm \to cs, \tau\nu$. In the MSSM the decay width for $H^\pm \to A\,W$ is very suppressed in most of the parameter

space [6–8], because the charged Higgs and the CP-odd Higgs are close to mass degeneracy.

The importance of the decays $H^\pm \to A_1 W$ and $H^\pm \to H_1 W$ in the NMSSM was first pointed out in [9]. Their branching ratios may be close to 100%, which can provide a clear signal at the LHC. Simulations of the process $pp \to t\bar{t}$ followed by $t \to H^\pm b$ and $H^\pm \to A_1 W$ have been performed for the NMSSM [10], CP conserving MSSM [76] and CP violating MSSM [77]. The partial width is given by

$$\Gamma(H^\pm \to A_1 W) = \frac{\alpha \cos^2\theta_A}{16 s_W^2 M_W^2 M_{H^\pm}^3} \lambda^{\frac{3}{2}} \left(M_{H^\pm}^2, M_{A_1}^2, M_W^2\right), \tag{13}$$

where $\lambda(x,y,z) = x^2+y^2+z^2-2(xy+xz+yz)$ is the two-body phase space function. The decay width of $H^\pm \to H_1 W$ can be obtained from (13) by replacing $\cos\theta_A$ by $g_{H^\pm W^\mp H_1}$ and M_{A_1} by M_{H_1}.

As can be seen from (13), the decay width of $H^\pm \to A_1 W$ is directly proportional to $\cos\theta_A$, which is the doublet component of A_1. This decay width can be substantially enhanced if A_1 is predominantly composed of doublet fields. However, even with a small doublet (large singlet) component of A_1 it is possible that $H^\pm \to A_1 W$ is the dominant decay mode. We perform a scan of the parameter space using the code [11, 12] (NMSSM-tools incorporates the LEP2 bounds for $4b$ and $6b$ final states) in order to quantify the importance of $H^\pm \to A_1 W$ and $H^\pm \to H_1 W$.

Hereafter we assume that all scalar superparticles share the same soft mass term $M_{\rm SUSY}$, and the ratios of gaugino masses satisfy $M_1 : M_2 : M_3 = 1 : 2 : 6$; the trilinear couplings are related to $M_{\rm SUSY}$ but the sign is not fixed, i.e. $A_{t,b} = \pm 2 M_{\rm SUSY}$. We scan the parameter space of the model by varying the free parameters within the following region:

$$\begin{aligned} \lambda &= [0,1]\,, \quad \kappa = [-1,1]\,, \quad \tan\beta = [0.2, 60]\,, \\ \mu &= [-1,1]\,\text{TeV}\,, \\ A_\lambda &= [-1.0, 1.0]\,\text{TeV}\,, \quad A_\kappa = [-1.0, 1.0]\,\text{TeV}\,, \\ M_{\rm SUSY} &= [0.2, 3]\,\text{TeV}\,, \quad M_1 = [0.07, 3]\,\text{TeV}\,. \end{aligned} \tag{14}$$

While varying these parameters, we take into account the experimental constraints on the MSSM spectrum, e.g., charged Higgs mass ≥ 80 GeV, chargino and scalar fermions $\gtrsim 100$ GeV. We also apply the full set of LEP constraints obtained from searches for neutral Higgs bosons decaying to final states like $Z2b$, $Z4b$, $6b$, 6τ, $Z2b2\tau$, $Z4\tau$, $2b2\tau$.

In Fig. 1 we display the branching ratios of $W^\pm A_1$, $\tau\nu$ and top–bottom modes. Before the opening of the $H^\pm \to tb$ channel, the full dominance of $W^\pm A_1$ over $\tau\nu$ requires a light $M_{A_1} \lesssim 100$ GeV, a large doublet component of A_1, and $\tan\beta$ not too large. Note that at large $\tan\beta$, ≈ 15–25, the $W^\pm A_1$ and $\tau\nu$ channels become comparable in size. Once the decay $H^\pm \to tb$ is open, it competes strongly with $W^\pm A_1$ for $\tan\beta \lesssim 15$. As can be seen from Fig. 1 upper left, the branching ratio of $H^\pm \to W^\pm A_1$ is less than 90%. It is interesting to see also that for $\cos^2\theta_A \lesssim 0.05$ there is not a single point with $\mathrm{Br}(H^\pm \to W^\pm A_1) \gtrsim 50\%$. Note also that at large $\tan\beta \gtrsim 25$, it is hard for $H^\pm \to W^\pm A_1$ to compete with $\tau\nu$ and top–bottom modes.

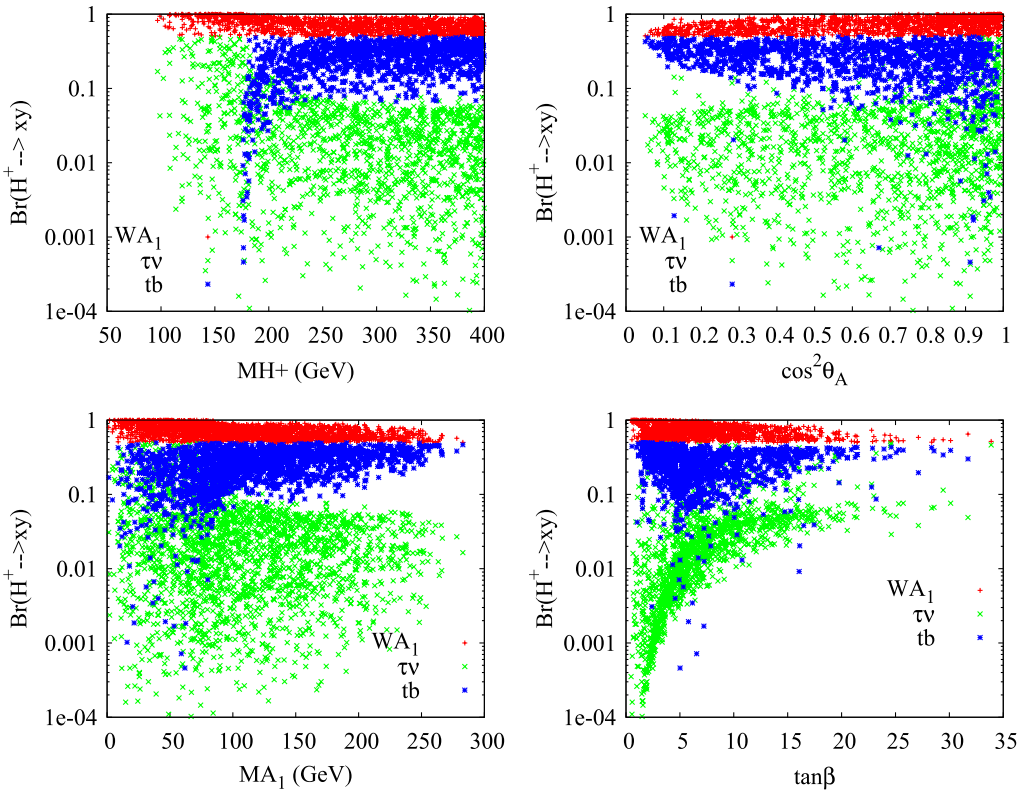

Fig. 1. Comparison of the branching ratios of $H^\pm \to \{W^\pm A_1, \tau\nu, tb\}$ as a function of $M_{H^\pm}$ (*upper left*), $\cos\theta_A$ (*upper right*), M_{A_1} (*lower left*) and $\tan\beta$ (*lower right*). In all panels only points with $\mathrm{Br}(H^\pm \to W^\pm A_1) \geq 50\%$ are selected

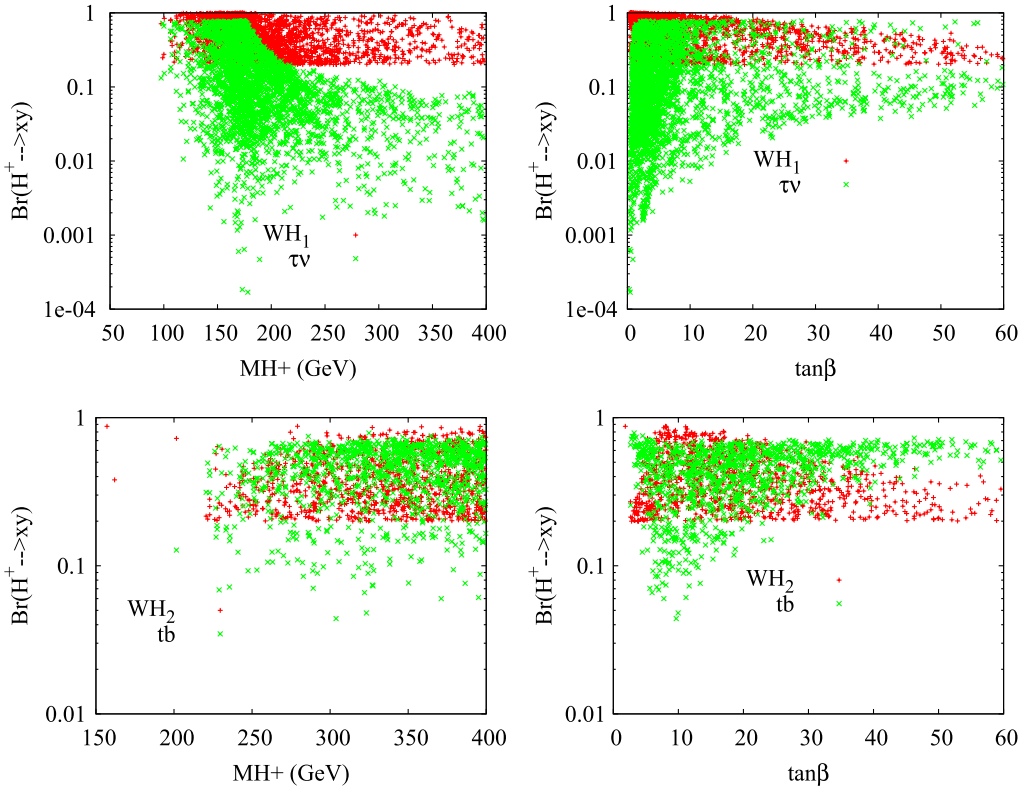

Fig. 2. Comparison of the branching ratios of $H^\pm \to \{W^\pm H_1, \tau\nu\}$ (*upper plots*) and $H^\pm \to \{W^\pm H_2, tb\}$ (*lower plots*) as a function of $M_{H^\pm}$ (*left*) and $\tan\beta$ (*right*). In all panels only points with $\mathrm{Br}(H^\pm \to W^\pm H_i) \geq 20\%$ are selected ($i = 1$ or 2)

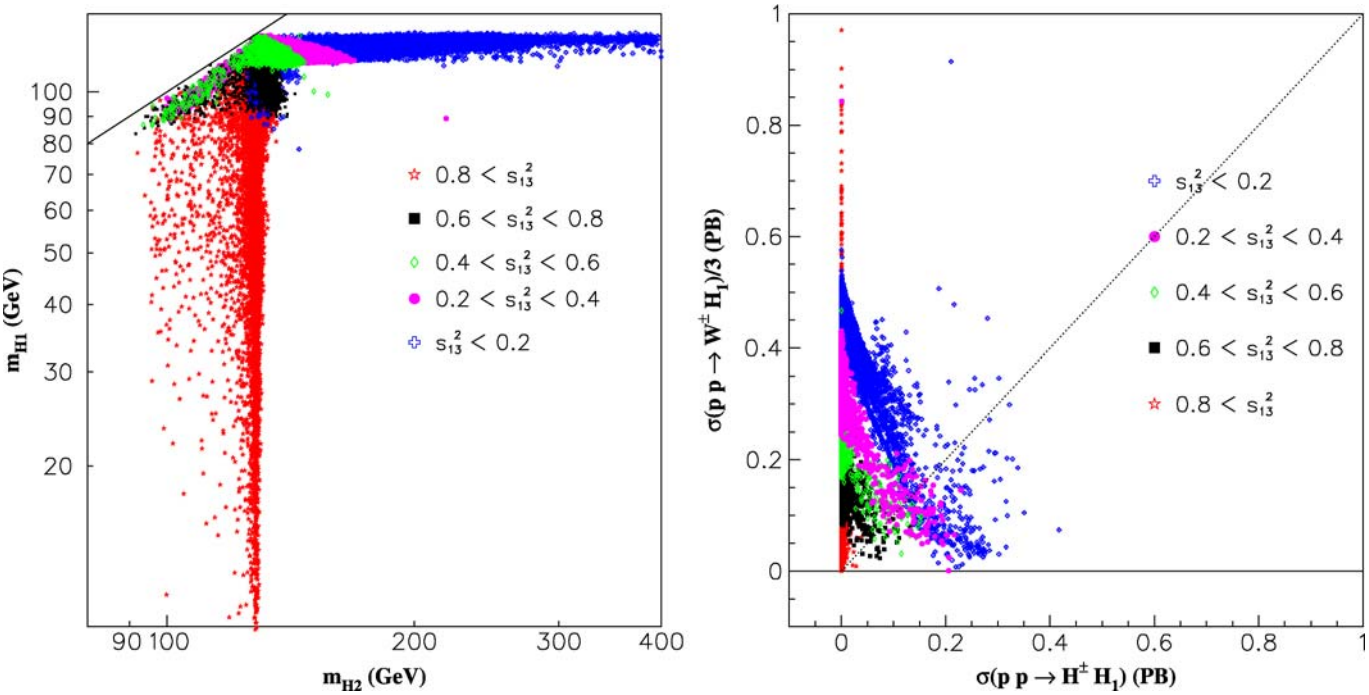

Fig. 3. *Left panel*: the comparison of m_{H_1} and m_{H_2} with respect to S^2_{13}. *Right panel*: the comparison of the cross section of the processes $pp \to W^\pm H_1$ and $pp \to H^\pm H_1$. For $\sigma(pp \to H^\pm H_1)$, we sum over $\sigma(pp \to H^+ H_1)$ and $\sigma(pp \to H^- H_1)$, while for $\sigma(pp \to W^\pm H_1)$ we sum over $\sigma(pp \to W^+ H_1)$ and $\sigma(pp \to W^- H_1)$. For the sake of comparison, we deliberately divide $\sigma(pp \to W^\pm H_1)$ by 3 due to the three helicity states of massive vector boson W

The cases of the analogous decays $H^\pm \to W^\pm H_{1,2}$ are displayed in Fig. 2 as a function of $M_{H^\pm}$ and $\tan\beta$. One can see from the upper right panel of Fig. 2 that $W^\pm H_1$ dominates over $\tau\nu$ only for moderate $\tan\beta$, $\lesssim 5$, and before opening of $H^\pm \to tb$ decay, which strongly competes with the $H^\pm \to W^\pm H_1$ mode.

From the lower panel of Fig. 2 one can see that the branching ratio for $H^\pm \to W^\pm H_2$ can only be larger than 20% for a charged Higgs mass larger than about 220 GeV. This is mainly due to the fact that m_{H_2} is most of the time larger than 140 GeV. It is clear that both $H^\pm \to W^\pm H_2$ and $H^\pm \to tb$ are of comparable size, except in the case of large $\tan\beta$, where $H^\pm \to tb$ mode dominates.

Importantly, we note that if $S^2_{13} \approx 1$, the second sum rule in (8) requires $g^2_{VVH_1} \approx 0$ and $g^2_{W^\pm H^\mp H_1} \approx 0$. In this case, $S^2_{i3} \approx 1$, both modes $H^\pm \to W^\pm H_{1,2}$ are suppressed and hence the full dominance of $W^\pm H_{1,2}$ requires a small S_{i3}.

In our numerical analysis we have explicitly checked that if H_1 is predominantly singlet, i.e., $S^2_{13} \gtrsim 0.9$, both couplings $g^2_{VVH_1}, g^2_{W^\pm H^\mp H_1} \lesssim 0.1$, in accordance with this sum rule. The larger S^2_{13} is, the smaller are the couplings $g^2_{VVH_1}$ and $g^2_{W^\pm H^\mp H_1}$. When $S^2_{13} \gtrsim 0.9$, H_1 is almost purely singlet and even a very light H_1 can be allowed by LEP experimental constraints. In this case, both the vertices of ZZH_1 and $f\bar{f}H_1$ are suppressed, as shown in Fig. 3a. In this case, the H_2 will be the standard-model-like Higgs boson and the coupling g_{VVH_2} can be large, as indicated by the first sum rule in (8) and demonstrated in Fig. 3a.

In the converse case when $S^2_{13} \approx 0 \to 0.1$, $g^2_{VVH_1}$ and $g^2_{W^\pm H^\mp H_1}$ have to share the quantity $1 - S^2_{13}$. Since H_1 is dominantly doublet the coupling $g_{W^\pm H^\mp H_1}$ can be maximal, and hence the branching ratio of $H^\pm \to W^\pm H_1$ can be large.

5.2 The cross sections for $pp \to H^\pm H_1$, $pp \to W^\pm H_1$ and $pp \to H^\pm A_1$ in the NMSSM

Searches for Higgs bosons at the LHC suffer from large QCD backgrounds. However, detailed studies have shown that multiple signals for the MSSM Higgs bosons are possible in a sizeable region of the $[\tan\beta, M_{H^\pm}]$ plane [78]. Many of these studies for the MSSM can be applied to the NMSSM with some caveats, which were discussed in Sect. 4. The most problematic region for $H^\pm$ discovery in the MSSM is for moderate values of $\tan\beta$, since the production mechanisms, which rely on a large bottom quark or top quark Yukawa coupling (e.g. $gb \to H^\pm t$) are least effective. Hence alternative mechanisms that could offer good detection prospects for $H^\pm$ at moderate values of $\tan\beta$ are desirable.

The cross sections for the pair production mechanisms $pp \to H^\pm A_1$ and $pp \to H^\pm H_1$ fall quickly with increasing scalar masses but for relatively light masses ($\lesssim 200$ GeV) they can provide promising signal rates that might enable their detection at the LHC. One common feature is that the produced scalars enjoy large transverse momenta, which are crucial for the trigger and event selection. The cross section for $pp \to W^\pm \to H^\pm A$ was first studied [13, 14] at both the LHC and Tevatron in the CP conserving MSSM for $M_A > 100$ GeV. The analogous process $pp \to H^\pm H_1$ for a very light H_1 with unsuppressed coupling $H_1 H^\pm W^\mp$ was studied in the 2HDM and the CP violating MSSM in [16] at the Tevatron. In [15] it was shown that $pp \to H^\pm h^0, H^\pm A^0$ can be important in specific regions of parameter space (i.e., very light h^0 and A^0) in the CP conserving MSSM.

In the NMSSM, if the coupling $H^\pm W^\mp A_1$ is sizeable, so will be the cross section for $pp \to W^\pm \to H^\pm A_1$ provided that $H^\pm$ and A_1 are not too heavy. The production mechanism $pp \to H^\pm A_1$ followed by the decay $H^\pm \to W^\pm A_1$ would give rise to a signal $W^\pm A_1 A_1 \to Wbbbb$ [16] or $W^\pm A_1 A_1 \to W\tau\tau\tau\tau$. The signature $W^\pm A_1 A_1 \to Wbbbb$ was simulated at the LHC in [17] in the context of the CP violating MSSM with the conclusion that a sizeable signal essentially free of background could be obtained. We use NMSSM-TOOLS1.1.1 to calculate the mass spectrum and couplings of the NMSSM Higgs bosons, and we link CTEQ6.1M PDF distribution to this code in order to calculate the cross sections of $pp \to H^\pm A_1$, $pp \to H^\pm H_1$ and $pp \to W^\pm H_1$. All cross sections are evaluated at a scale that is the sum of the masses in final states and do not include next-to-leading order QCD enhancement factors (K factors) of around $1.2 \to 1.3$ [13, 14, 79, 80].

For our numerical analysis, we have done a systematic scan with NMSSM-TOOLS1.1.1 [11, 12]. Firstly, we explore the phenomenological implication of the sum rule (8) with Fig. 3b. There are several comments in order.

1) All points in Fig. 3b respect the following constraint $M_{H^\pm} \gtrsim M_W$; this leads to a smaller cross section for $\sigma(pp \to H^\pm H_1)$.
2) As S^2_{13} increases both processes are suppressed due to the decrease of the couplings $W^\mp W^\pm H_1$ and $W^\mp H^\pm H_1$.
3) When $S^2_{13} > 0.8$, H_1 is dominated by a singlet component, it can be very light – see Fig. 3a. In this case, according to sum rule (8), the vertex VVH_1 suffers severe suppression. However, some points with large $\sigma(pp \to W^\pm H_1)$ arise due to the fact that a very light H_1 is allowed.

In Fig. 4a we study the cross section of $pp \to H^\pm H_1$ at the LHC and select points which simultaneously satisfy the following conditions:

$$\sigma(pp \to H^\pm H_1) > 0.1\,\text{pb}\,, \quad \text{Br}(H^\pm \to W^\pm A_1) > 0.5\,. \tag{15}$$

We require points in parameter space with cross sections larger than 0.1 pb as a conservative threshold of the observability for this channel at the LHC. From the figure it is clear that $\sigma(pp \to H^\pm H_1) < 0.5$ pb when the charged Higgs boson decays dominantly to $W^\pm A_1$.

In Fig. 4b, we study the cross section of $pp \to W^\pm H_1$ at LHC and select points which satisfy the following conditions:

$$\sigma(pp \to W^\pm H_1) > 0.1\,\text{pb}\,, \quad \text{Br}(H_1 \to A_1 A_1) > 0.5\,. \tag{16}$$

The typical cross section for $\sigma(pp \to W^\pm H_1)$ is around a few pb, which is considerably larger than $\sigma(pp \to H^\pm H_1)$. The larger cross sections correspond to the larger branching ratios for $H_1 \to A_1 A_1$ ($> 90\%$). The numerical results

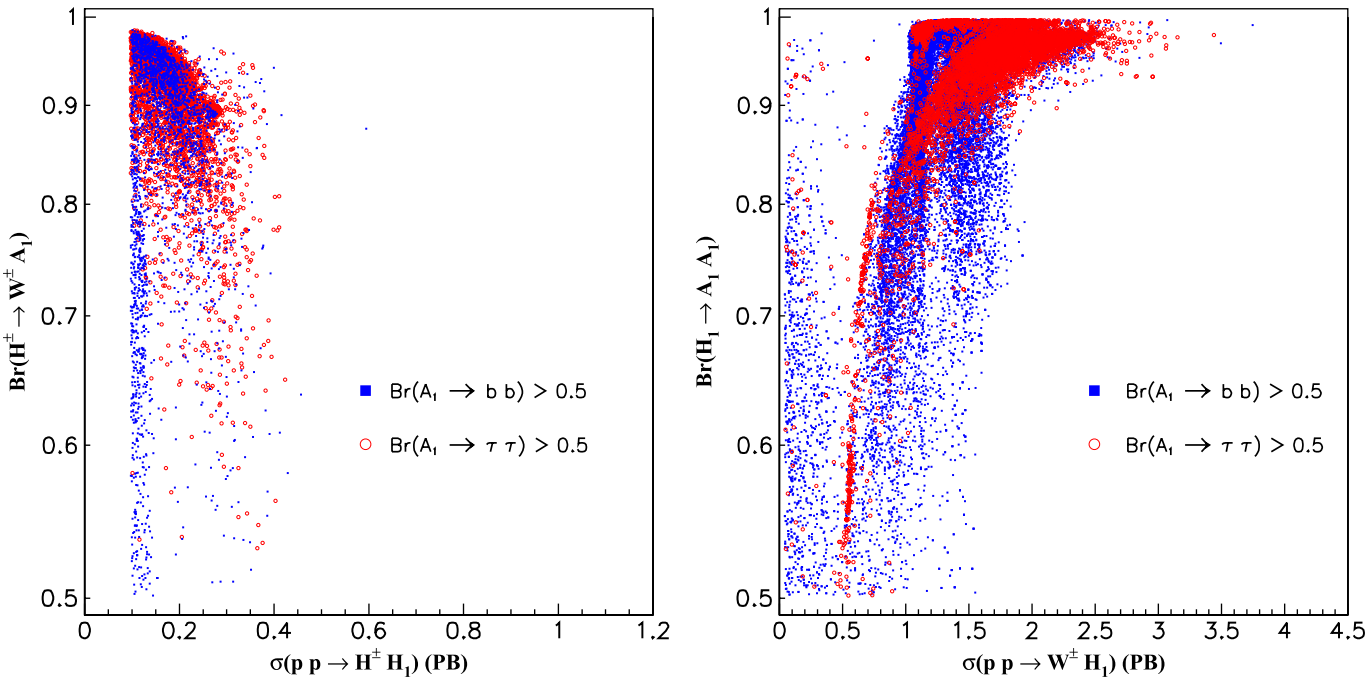

Fig. 4. *Left panel*: points selected with the condition given in (15). *Right panel*: points selected with the condition given in (16). For $\sigma(pp \to H^{\pm}H_1)$ we sum over $\sigma(pp \to H^{+}H_1)$ and $\sigma(pp \to H^{-}H_1)$; for $\sigma(pp \to W^{\pm}H_1)$ we sum over $\sigma(pp \to W^{+}H_1)$ and $\sigma(pp \to W^{-}H_1)$. We show the two decay modes of A_1: $A_1 \to b\bar{b}$, and $A_1 \to \tau\bar{\tau}$, which corresponds to two mass regions: $2m_b < M_{A_1} < m_{H_1}/2$, and $2m_\tau < M_{A_1} < 2m_b$, respectively

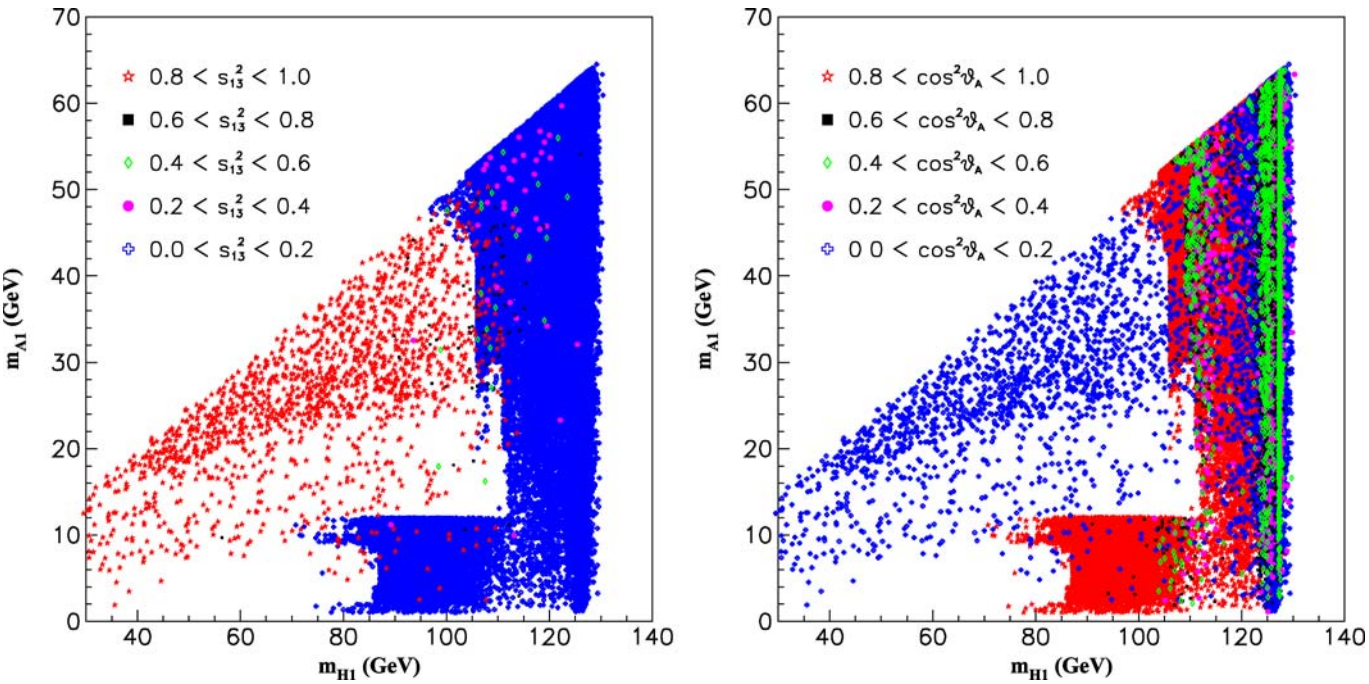

Fig. 5. Parameter space satisfying $\mathrm{Br}(H_1 \to A_1A_1) \geq 0.5$ in the plane $[m_{H_1}, m_{A_1}]$. The components of both H_1 and A_1 are displayed

in Fig. 4b are in good agreement with analogous results presented in [46].

In Fig. 5 we analyze the components of H_1 and A_1. Points which satisfy the following condition are selected:

$$\mathrm{Br}(H_1 \to A_1A_1) \geq 0.5\,. \tag{17}$$

As expected, when both H_1 and A_1 are dominantly composed of doublet fields the region of light Higgs bosons is

ruled out from searches for $e^+e^- \to ZH_1 \to Z2A_1 \to Z4b$, and m_{H_1} should be heavier than around $100 \sim 110$ GeV. When $M_{A_1} \lesssim 2m_b$, m_{H_1} can be lighter than 100 GeV due to the fact that the LEP2 sensitivity to the channel $e^+e^- \to Z4\tau$ was less robust than that for $e^+e^- \to Z4b$. Interestingly, when both H_1 and A_1 are mainly singlet and hence the vertex of VVH_1 is greatly suppressed, much lighter values for m_{H_1} ($\lesssim 80$ GeV) are still allowed, as shown by points with red stars in Fig. 5a and blue crosses in Fig. 5b.

This process, $pp \to H^\pm A_1 \to W^\pm A_1 A_1$, leads to the same signature as the process $pp \to WH_1 \to WA_1A_1 \to Wbbbb$. The latter has been simulated in [18] and also offers very good detection prospects. We will compare the magnitude of these two distinct mechanisms, which lead to the same $Wbbbb$ signature. In addition, the mechanism $pp \to H^\pm H_1$ followed by the decay $H^\pm \to W^\pm A_1$ would also lead to the same final state $W^\pm A_1 H_1 \to Wbbbb$. We will concentrate on the scenario where $H_1 \to A_1A_1$ is large and thus $H_1 \to b\bar{b}$ will be kinematically suppressed. We will discuss the magnitude of $pp \to H^\pm H_1 \to W^\pm A_1 H_1 \to Wbbbb$ later.

In Fig. 6a we study the process $pp \to H^\pm A_1$ by choosing points that satisfy the following conditions:

$$\sigma(pp \to H^\pm A_1) > 0.1 \text{ pb}\,, \quad \text{Br}(H^\pm \to W^\pm A_1) > 0.5\,. \tag{18}$$

It is apparent that the magnitude of $\sigma(pp \to H^\pm A_1)$ can reach a few pb and thus is within the detection capability of the LHC. The analysis of [17] (for the CP violating MSSM) suggests that $\sigma(pp \to H^\pm A_1) \gtrsim 0.1$ pb with a large $\text{Br}(H^\pm \to W^\pm A_1)$ would be sufficient for an observable $Wbbbb$ signal at the LHC. Most strikingly, the cross section of the process $pp \to H^\pm A_1$ can be comparable to that of $pp \to W^\pm H_1$.

The majority of the points in Fig. 6a correspond to the parameter space where $\tan\beta$ is located in the range $0.2 \lesssim \tan\beta \lesssim 20$. As seen in the previous section, when $\tan\beta \gtrsim 20$ the decay channel $H^\pm \to \tau^\pm \nu_\tau$ (or $H^\pm \to tb$) will dominate over $H^\pm \to W^\pm A_1$. It is evident from Fig. 6a that there are plenty of points with $\sigma(pp \to H^\pm A_1) \gtrsim 0.1$ pb and $\text{Br}(H^\pm \to W^\pm A_1) \gtrsim 90\%$.

In Fig. 6b we show the dependence of $\sigma(pp \to H^\pm A_1)$ on $\tan\beta$ and $\cos\theta_A$. The figure clearly shows that when A_1 is mainly doublet the cross section $\sigma(pp \to H^\pm A_1)$ can reach a few pb. Importantly, the cross section can be sizeable in the whole region $1 < \tan\beta < 30$, and thus this mechanism can be applied to the region $5 \lesssim \tan\beta \lesssim 20$, for which $H^\pm$ discovery in the conventional production mechanisms (which utilize the t and b quark Yukawa couplings) is least effective. Thus $H^\pm$ production via $pp \to H^\pm A_1$ might offer the best prospects for the detection of a light NMSSM charged Higgs boson in the region of intermediate $\tan\beta$. It is clear from Fig. 6b that there are no points at all with $0 \lesssim \cos^2\theta_A \lesssim 0.4$, the reason being that such points do not satisfy the requirement $\sigma(pp \to H^\pm A_1) \gtrsim 0.1$ pb.

Figure 7 shows the dependence of $\sigma(pp \to H^\pm H_1(A_1))$ on $m_{H_1}(m_{A_1}) + m_{H^\pm}$. Points in Fig. 7a satisfy the conditions given in (15), while points in Fig. 7b satisfy the conditions given in (18). Clearly the points with large cross section correspond to the region in the parameter space

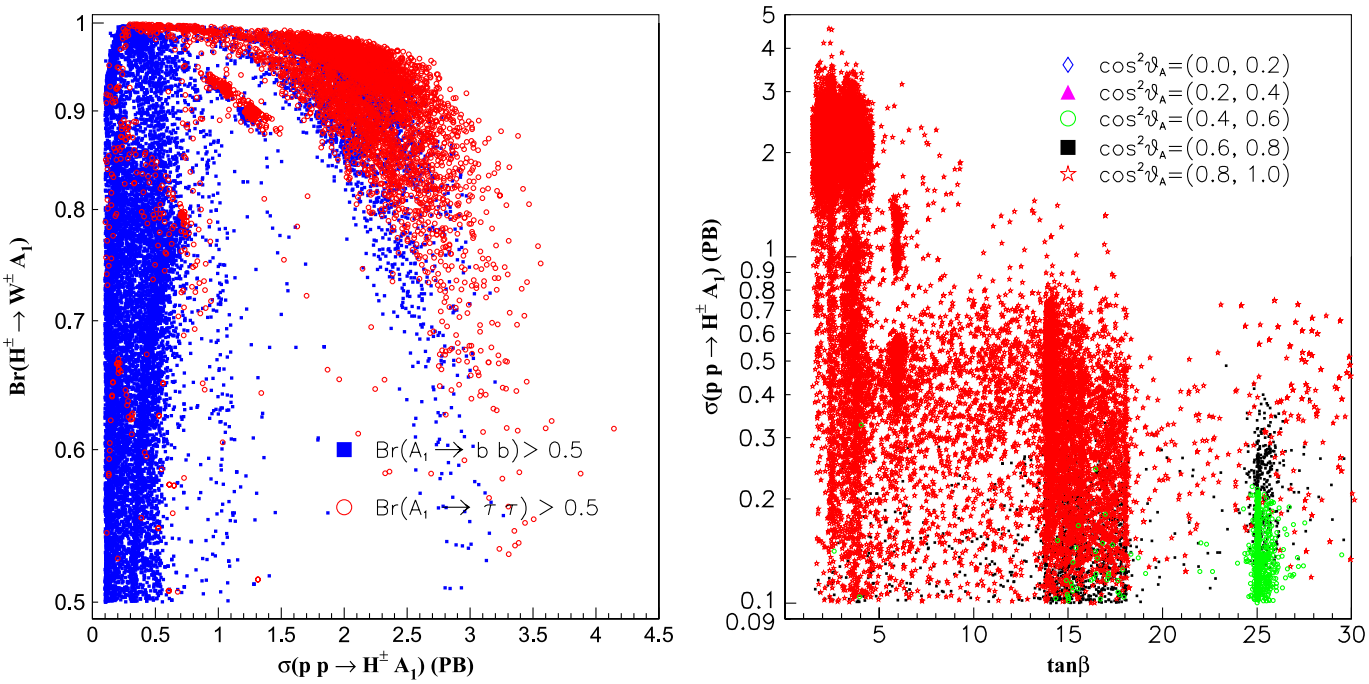

Fig. 6. *Left panel*: points in the plane $[\sigma(pp \to H^\pm A_1), \text{Br}(H^\pm \to A_1 W]$ that satisfy the conditions given in (18). For $\sigma(pp \to H^\pm A_1)$ we sum over $\sigma(pp \to H^+ A_1)$ and $\sigma(pp \to H^- A_1)$. We show the two decay modes of A_1: $A_1 \to b\bar{b}$ and $A_1 \to \tau\bar{\tau}$, which corresponds to the two mass regions $2m_b < M_{A_1} < m_{H_1}/2$ and $2m_\tau < M_{A_1} < 2m_b$, respectively. *Right panel*: the dependence of $\sigma(pp \to H^\pm A_1)$ on both $\tan\beta$ and $\cos\theta_A$ are displayed

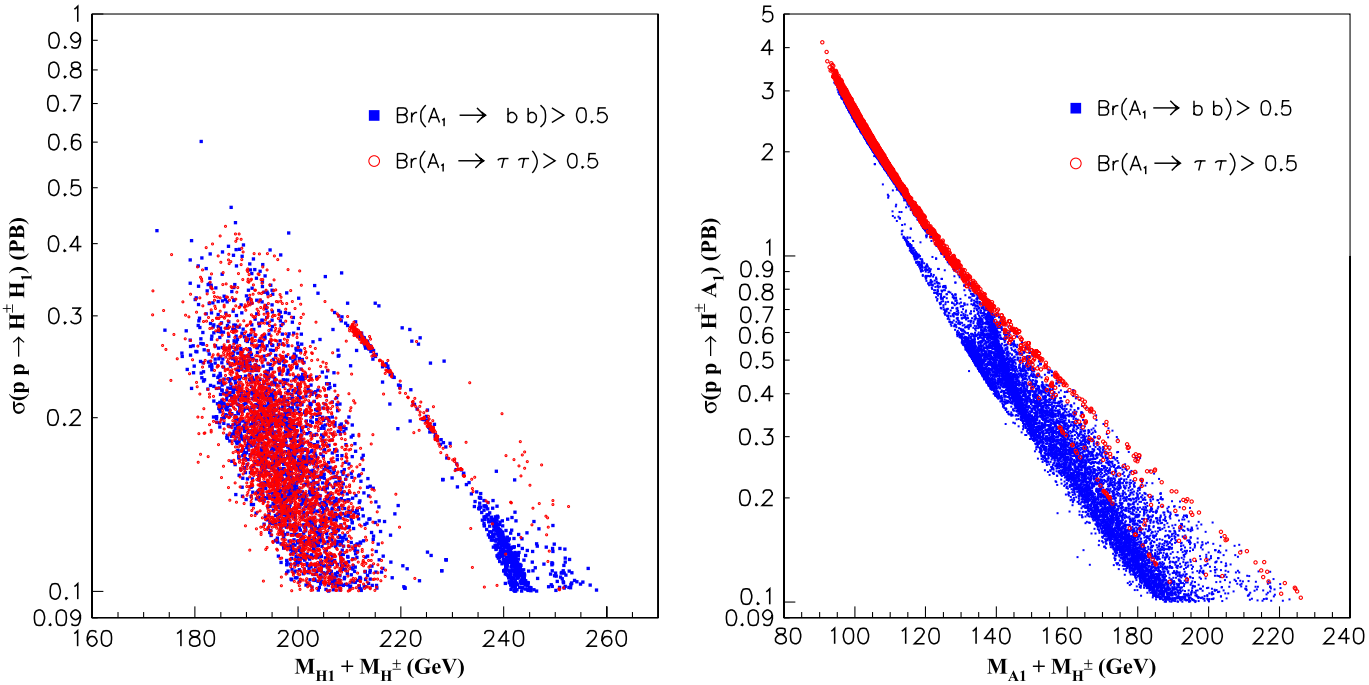

Fig. 7. *Left panel*: the cross section of $pp \to H^{\pm}H_1$ against $M_{H_1} + M_{H^{\pm}}$; all points satisfy the condition in (15). *Right panel*: the cross section of $pp \to H^{\pm}A_1$ against $M_{A_1} + M_{H^{\pm}}$; all points satisfy the condition in (18). We show the two decay modes of A_1: $A_1 \to b\bar{b}$ and $A_1 \to \tau\bar{\tau}$, which corresponds to the two mass regions $2m_b < M_{A_1} < m_{H_1}/2$ and $2m_\tau < M_{A_1} < 2m_b$, respectively

where both $H^{\pm}$ and $H_1(A_1)$ are light and the couplings $W^{\mp}H^{\pm}H_1$ and $W^{\mp}H^{\pm}A_1$ are near maximal. In Fig. 7b, it is evident that the cross section for $pp \to H^{\pm}A_1$ can reach a few pb when A_1 is as light as 10 GeV. In contrast, in Fig. 7a one can see that there are only points for $m_{H_1} + m_{H^{\pm}} \gtrsim 170$ GeV which corresponds to $m_{H^{\pm}} \gtrsim 80$ GeV and $m_{H_1} \gtrsim 90$ GeV. The lack of sample points with a large cross section for $pp \to H^{\pm}H_1$ is due to difficulties in finding points with relatively light H_1 and $H^{\pm}$ (i.e., $m_{H_1} + m_{H^{\pm}} \lesssim 170$ GeV), which can satisfy the experimental constraints.

As emphasized earlier, the processes $pp \to H^{\pm}A_1$ and $pp \to VH_1$ could lead to the same final state, $Wbbbb$ or $W\tau\tau\tau\tau$. Hence a numerical comparison of their cross sections is of particular interest and is shown in Fig. 8, where all points satisfy the following conditions:

$$\sigma(pp \to H^{\pm}A_1) > 0.1\,\text{pb}\,, \quad \sigma(pp \to W^{\pm}H_1) > 0.1\,\text{pb}\,. \tag{19}$$

Superimposed on Fig. 8a and b are the main decay modes of the charged Higgs boson and the decay neutral Higgs boson H_1, respectively. We further impose the following conditions:

$$\text{Br}(H^{\pm} \to W^{\pm}A_1) > 0.5\,, \quad \text{Br}(H_1 \to A_1A_1) > 0.5\,, \tag{20}$$

and the surviving points are displayed in Fig. 9a. Importantly, there are many points where the two cross sections are of comparable size. We note that for these points in Fig. 9a the pseudoscalar A_1 can be both R-axion-like or a mixture of the three allowed basic axions. If the magnitude of the cross sections of both $pp \to H^{\pm}A_1$ and $pp \to VH_1$ are similar, then the interference of the two channels (i.e., the same $Wbbbb$ signature arising from distinct production mechanisms) should be taken into account. We have neglected such effects in the present study.

We now discuss whether the $Wbbbb$ signatures can be distinguished experimentally by comparing the strategies adopted in [17] (for $pp \to H^{\pm}A^0$) and [18] (for $pp \to W^{\pm}H_1$). In order to reconstruct the peak of the CP-even Higgs H_1, one can select events with a charged lepton and four tagged b quark jets as shown in [18]. This enables both a clean Higgs signal with high significance and a measurement of M_{H_1} given by the invariant mass of the four b quark jets, m_{4b}. The process $pp \to H^{\pm}A_1$ might be an irreducible background but presumably could be significantly suppressed with the aforementioned cut on m_{4b}, e.g., $m_{H_1} - 15\,\text{GeV} < m_{4b} < m_{H_1} + 15\,\text{GeV}$.

Regarding detection of $pp \to H^{\pm}A^0$, it was demonstrated in [17] (for the analogous process $pp \to H^{\pm}H_1 \to WH_1H_1$ in the CP violating MSSM) that the mass of $H^{\pm}$ can be reconstructed. This is achieved by defining a transverse mass (M_{T}), which is a function of the momenta of the two secondary b jets (i.e., those originating from the decay $H^{\pm} \to A_1W \to Wbb$) and the momenta of the lepton and missing energy coming from the W boson. It was shown that M_{T} is sensitive to the underlying charged Higgs mass and thus can be used for the determination of $M_{H^{\pm}}$. The pair of b jets from $pp \to W^{\pm}H_1$ might be an irreducible background but presumably could be suppressed with a cut on M_{T}.

To reconstruct the peak of the light CP-odd neutral Higgs A_1 one can require events with four tagged b jets, construct the three possible double pairings of $b\bar{b}$ invari-

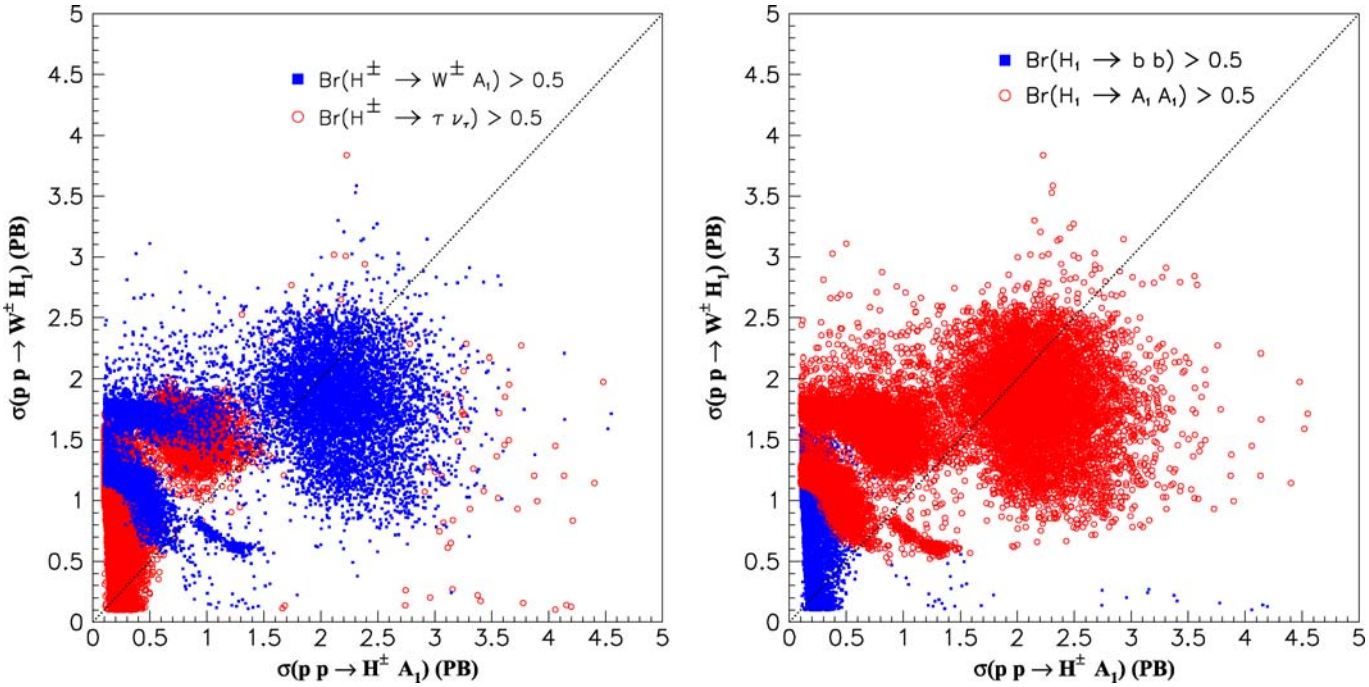

Fig. 8. *Left panel*: comparison of $\sigma(pp \to H^{\pm}A_1)$ and $\sigma(pp \to W^{\pm}H_1)$ with two $H^{\pm}$ decay modes. *Right panel*: comparison of $\sigma(pp \to H^{\pm}A_1)$ and $\sigma(pp \to W^{\pm}H_1)$ with two H_1 decay modes. The *dotted line* corresponds to $\sigma(pp \to W^{\pm}H_1) = \sigma(pp \to H^{\pm}A_1)$

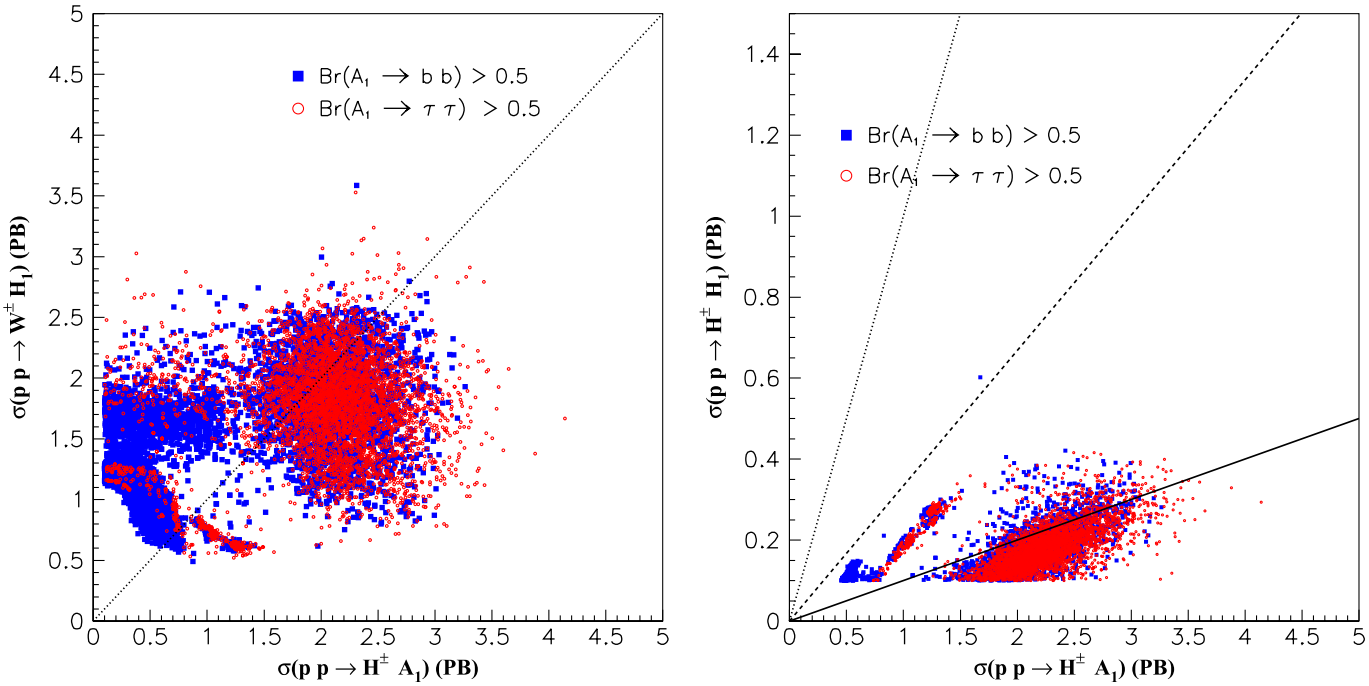

Fig. 9. *Left panel*: comparison of $\sigma(pp \to H^{\pm}A_1)$ and $\sigma(pp \to W^{\pm}H_1)$ with different A_1 decay modes. Points are selected with the condition given in (19)–(20). *Right panel*: comparison of $\sigma(pp \to H^{\pm}A_1)$ and $\sigma(pp \to H^{\pm}H_1)$ with the same set of points. The *dotted line* corresponds to $\sigma(pp \to H^{\pm}A_1) = \sigma(pp \to H^{\pm}H_1)$; the *dashed line* corresponds to $\sigma(pp \to H^{\pm}A_1) = 3\sigma(pp \to H^{\pm}H_1)$; the *solid line* corresponds to $\sigma(pp \to H^{\pm}A_1) = 10\sigma(pp \to H^{\pm}H_1)$

ant masses, and then select the pairing giving the least difference between the two $b\bar{b}$ invariant masses values [17]. $W4b$ signatures from the process $pp \to W^{\pm}H_1$ also contribute constructively to the reconstruction of A_1. Thus we conclude that it is promising to reconstruct the peaks of the CP-even neutral Higgs (H_1), charged Higgs ($H^{\pm}$) and CP-odd neutral Higgs (A_1) and thus experimentally distinguish the $Wbbbb$ signatures arising from the two distinct

production mechanisms. We defer a detailed simulation to future work.

Finally, we also compare the cross sections of $pp \to H^\pm A_1$ and $pp \to H^\pm H_1$ in Fig. 9b. The points are from the same data sample used in Fig. 9a. It is clear that $\sigma(pp \to H^\pm A_1)$ is around one order of magnitude larger than $\sigma(pp \to H^\pm H_1)$, and the underlying reason is that $M_{H_1} > 2M_{A_1}$. Consequently, $pp \to H^\pm H_1 \to W^\pm A_1 H_1 \to Wbbbb$ will also be suppressed and can be safely neglected. Another interesting feature from Fig. 9b is that points satisfying the conditions listed in (20) lead to A_1 composed mainly of the doublet fields. The conditions in (20) together with the dominance of H_1 by doublet component (small S_{13}) can give large cross sections for both channels.

6 Conclusion

In summary, we have studied the phenomenology of light charged Higgs bosons in the framework of NMSSM. We performed a comprehensive study of the magnitude of the branching ratios for the decays $H^\pm \to W^\pm A_1$ and $H^\pm \to W^\pm H_1$ (first considered in [9]). It was shown that such decays can dominate over the standard decays $H^\pm \to \tau^\pm \nu$ and $H^\pm \to tb$ both below and above the top–bottom threshold. This is due to the fact that A_1 can have a large doublet component and a small mass. Large branching ratios for $H^\pm \to W^\pm A_1$ and $H^\pm \to W^\pm H_1$ would affect the anticipated search potential for $H^\pm$ at the LHC.

We also studied the production process $pp \to H^\pm A_1$ and showed that sizeable cross sections (> 1 pb) are possible. We compared the magnitude of the cross sections for both $pp \to H^\pm A_1$ and the Higgsstrahlung process $pp \to W^\pm H_1$ and showed that they can be of similar size. If $H^\pm$ and H_1 decay via $H^\pm \to W^\pm A_1$ and $H_1 \to A_1 A_1$, respectively, the above two processes would lead to the same final state, $Wbbbb$ or $W\tau\tau\tau\tau$. We stressed that the interference term for $Wbbbb$ and $W\tau\tau\tau\tau$ might not be negligible and should be taken into account in any simulation study. In particular, the signature $Wbbbb$ affords promising detection prospects at the LHC, and we discussed how to distinguish the distinct contributions from $pp \to H^\pm A_1$ and $pp \to W^\pm H_1$ by using appropriate cuts.

It is known that intermediate values of $\tan\beta$ (e.g., $5 < \tan\beta < 20$) are most problematic for the discovery of $H^\pm$ at the LHC, since the $H^\pm tb$ Yukawa coupling (which is employed in the conventional production processes) takes its lowest values. In such a region the process $pp \to H^\pm A_1$ can have a sizeable cross section if $m_{H^\pm} + m_{A_1} < 200$ GeV. Therefore, we propose $pp \to H^\pm A_1$ as a unique mechanism to probe the parameter space of intermediate $\tan\beta$ and light charged Higgs boson in the NMSSM.

Acknowledgements. We would like to thank Kingman Cheung for useful discussions. A.A. is supported by the National Science Council of R.O.C. under Grant No. NSC96-2811-M-008-020. Q.S.Y. is supported by the National Science Council of R.O.C. under Grant No. NSC 95-2112-M-007-001 and 96-2628-M-007-002-MY3. A.G.A. is supported by National Cheng Kung University Grant No. OUA 95-3-2-057.

References

1. J.E. Kim, H.P. Nilles, Phys. Lett. B **138**, 150 (1984)
2. Y. Nir, Phys. Lett. B **354**, 107 (1995) [hep-ph/9504312]
3. M. Cvetic, P. Langacker, Phys. Rev. D **54**, 3570 (1996) [hep-ph/9511378]
4. R. Dermisek, J.F. Gunion, Phys. Rev. Lett. **95**, 041 801 (2005)
5. R. Dermisek, J.F. Gunion, arXiv:0705.4387 [hep-ph]
6. S. Moretti, W.J. Stirling, Phys. Lett. B **347**, 291 (1995)
7. S. Moretti, W.J. Stirling, Phys. Lett. B **366**, 451 (1996)
8. A. Djouadi, J. Kalinowski, P.M. Zerwas, Z. Phys. C **70**, 435 (1996)
9. M. Drees, E. Ma, P.N. Pandita, D.P. Roy, S.K. Vempati, Phys. Lett. B **433**, 346 (1998)
10. M. Drees, M. Guchait, D.P. Roy, Phys. Lett. B **471**, 39 (1999)
11. U. Ellwanger, J.F. Gunion, C. Hugonie, JHEP **0502**, 066 (2005)
12. http://www.th.u-psud.fr/NMHDECAY/nmssmtools.html
13. S. Kanemura, C.P. Yuan, Phys. Lett. B **530**, 188 (2002)
14. Q.H. Cao, S. Kanemura, C.P. Yuan, Phys. Rev. D **69**, 075 008 (2004)
15. A. Belyaev, Q.H. Cao, D. Nomura, K. Tobe, C.P. Yuan, arXiv:hep-ph/0609079
16. A.G. Akeroyd, Phys. Rev. D **68**, 077 701 (2003)
17. D.K. Ghosh, S. Moretti, Eur. Phys. J. C **42**, 341 (2005)
18. K. Cheung, J. Song, Q.S. Yan, Phys. Rev. Lett. **99**, 031 801 (2007) hep-ph/0703149
19. M. Drees, Int. J. Mod. Phys. A **4**, 3635 (1989)
20. T. Elliott, S.F. King, P.L. White, Phys. Rev. D **49**, 2435 (1994)
21. F. Franke, H. Fraas, Int. J. Mod. Phys. A **12**, 479 (1997)
22. D.J. Miller, R. Nevzorov, P.M. Zerwas, Nucl. Phys. B **681**, 3 (2004)
23. Chapter 4 in E. Accomando et al., arXiv:hep-ph/0608079
24. U. Ellwanger, J.F. Gunion, C. Hugonie, S. Moretti, arXiv:hep-ph/0401228
25. S.F. King, P.L. White, Phys. Rev. D **53**, 4049 (1996)
26. B.A. Dobrescu, K.T. Matchev, JHEP **0009**, 031 (2000) [hep-ph/0008192]
27. D.J. Miller, R. Nevzorov, arXiv:hep-ph/0309143
28. L.J. Hall, T. Watari, Phys. Rev. D **70**, 115 001 (2004) [hep-ph/0405109]
29. D.J. Miller, S. Moretti, R. Nevzorov, arXiv:hep-ph/0501139
30. R.D. Peccei, H.R. Quinn, Phys. Rev. Lett. **38**, 1440 (1977)
31. J.R. Ellis, J.F. Gunion, H.E. Haber, L. Roszkowski, F. Zwirner, Phys. Rev. D **39**, 844 (1989)
32. M. Masip, R. Munoz-Tapia, A. Pomarol, Phys. Rev. D **57**, 5340 (1998).
33. L. Cavicchia, R. Franceschini, V.S. Rychkov, arXiv:0710.5750 [hep-ph]
34. R. Harnik, G.D. Kribs, D.T. Larson, H. Murayama, Phys. Rev. D **70**, 015 002 (2004)
35. S. Chang, C. Kilic, R. Mahbubani, Phys. Rev. D **71**, 015 003 (2005)

36. A. Delgado, T.M.P. Tait, JHEP **0507**, 023 (2005)
37. A. Birkedal, Z. Chacko, Y. Nomura, Phys. Rev. D **71**, 015 006 (2005)
38. D.P. Roy, Mod. Phys. Lett. A **19**, 1813 (2004)
39. A.G. Akeroyd, S. Baek, Phys. Lett. B **525**, 315 (2002)
40. D. Eriksson, S. Hesselbach, J. Rathsman, arXiv:hep-ph/0612198
41. J.F. Gunion, H.E. Haber, T. Moroi, At least one of the Higgs bosons of the next-to-minimal supersymmetric: in the Proc. of 1996 DPF/DPB Summer Study on New Directions for High-Energy Physics (Snowmass 96), Snowmass, Colorado, 25 Juni–12 July 1996, LTH095 [arXiv:hep-ph/9610337]
42. B.A. Dobrescu, G.L. Landsberg, K.T. Matchev, Phys. Rev. D **63**, 075 003 (2001)
43. U. Ellwanger, J.F. Gunion, C. Hugonie, arXiv:hep-ph/0111179
44. U. Ellwanger, J.F. Gunion, C. Hugonie, S. Moretti, arXiv:hep-ph/0305109
45. U. Ellwanger, J.F. Gunion, C. Hugonie, JHEP **0507**, 041 (2005)
46. S. Moretti, S. Munir, P. Poulose, Phys. Lett. B **644**, 241 (2007)
47. R. Dermisek, J.F. Gunion, Phys. Rev. D **73**, 111 701 (2006)
48. R. Dermisek, J.F. Gunion, Phys. Rev. D **75**, 075 019 (2007)
49. P.W. Graham, A. Pierce, J.G. Wacker, arXiv:hep-ph/0605162
50. M. Carena, T. Han, G.Y. Huang, C.E.M. Wagner, arXiv:0712.2466 [hep-ph]
51. J.R. Forshaw, J.F. Gunion, L. Hodgkinson, A. Papaefstathiou, A.D. Pilkington, arXiv:0712.3510 [hep-ph]
52. A. Arhrib, K. Cheung, T.J. Hou, K.W. Song, JHEP **0703**, 073 (2007)
53. R. Dermisek, J.F. Gunion, B. McElrath, Phys. Rev. D **76**, 051 105 (2007)
54. E. Fullana, M.A. Sanchis-Lozano, Phys. Lett. B **653**, 67 (2007)
55. R.M. Godbole, Light charged Higgs in CP-violating MSSM and NMSSM: in Proc. of IPM School and Conference on Lepton and Hadron Physics (IPM-LHP06), Tehran, Iran, 15–20 May 2006, p. 0016 [arXiv:hep-ph/0701193]
56. S. Bertolini, F. Borzumati, A. Masiero, G. Ridolfi, Nucl. Phys. B **353**, 591 (1991)
57. T. Hurth, Rev. Mod. Phys. **75**, 1159 (2003)
58. F. Borzumati, C. Greub, T. Hurth, D. Wyler, Phys. Rev. D **62**, 075 005 (2000)
59. K. Ikado et al., Phys. Rev. Lett. **97**, 251 802 (2006)
60. K. Ikado et al., arXiv:0705.1820 [hep-ex]
61. BABAR Collaboration, G. Nardo et al., arXiv:0708.2260 [hep-ex]
62. W.S. Hou, Phys. Rev. D **48**, 2342 (1993)
63. A.G. Akeroyd, S. Recksiegel, J. Phys. G **29**, 2311 (2003)
64. H. Itoh, S. Komine, Y. Okada, Prog. Theor. Phys. **114**, 179 (2005)
65. G. Isidori, P. Paradisi, Phys. Lett. B **639**, 499 (2006)
66. F. Domingo, U. Ellwanger, arXiv:0710.3714 [hep-ph]
67. F. Borzumati, A. Djouadi, Phys. Lett. B **549**, 170 (2002)
68. A.G. Akeroyd, Nucl. Phys. B **544**, 557 (1999)
69. A.G. Akeroyd, A. Arhrib, E. Naimi, Eur. Phys. J. C **20**, 51 (2001)
70. A.G. Akeroyd, A. Arhrib, E.M. Naimi, Eur. Phys. J. C **12**, 451 (2000)
71. A.G. Akeroyd, A. Arhrib, E.M. Naimi, Eur. Phys. J. C **14**, 371 (2000)
72. J.L. Diaz-Cruz, J. Hernandez-Sanchez, S. Moretti, A. Rosado, arXiv:0710.4169 [hep-ph]
73. DELPHI Collaboration, J. Abdallah et al., Eur. Phys. J. C **34**, 399 (2004)
74. OPAL Collaboration, Phys. Note PN445 (2000)
75. OPAL Collaboration, Phys. Note PN472 (2001)
76. S. Moretti, Phys. Lett. B **481**, 49 (2000)
77. D.K. Ghosh, R.M. Godbole, D.P. Roy, Phys. Lett. B **628**, 131 (2005)
78. K.A. Assamagan, Y. Coadou, A. Deandrea, Eur. Phys. J. C **4**, 9 (2002)
79. T. Han, S. Willenbrock, Phys. Lett. B **273**, 167 (1991)
80. M. Spira, Fortschr. Phys. **46**, 203 (1998)